



Research Article

Finite difference method for electric field optimization in high voltage power transformer bushings using engineering simulation and 3D design program

Nihat Pamuk ^{a,*} 

^aZonguldak Bülent Ecevit University, Department of Electric Electronic Engineering, Zonguldak, 67100, Turkey

ARTICLE INFO

Article history:

Received 07 July 2020

Revised 29 September 2020

Accepted 08 October 2020

Keywords:

Electric field distribution

Finite difference method

Optimization

Power transformer bushing

3D design

ABSTRACT

The electric field optimization minimizing the field strength on an electrode surface and providing its uniformity is important in designing high voltage power transformer bushings and other apparatus from the viewpoint of efficient utilization of the electric field space. The high voltage power transformer bushing with cylinder electrode system has been designed and tested in this investigation. It was found that the insulation method of the cylinder electrode was the most important factor to lower streamer initiation voltage. The optimized design uses both internal and external elements for electric stress grading at critical parts of the bushing. Applying optimization theory based on charge simulation method, the author developed a computation program for electric field automatic optimization in 3D dielectric axisymmetric field. The results of the computation realized some excellent electrode profiles with uniform electric field distribution. Moreover, the discrepancy from the electric field uniformity on 3D dimensional profile caused by applying it to an axisymmetric electrode was discussed. Then a new electrode with uniform field distribution was obtained by using the computation program for optimization.

© 2021, Advanced Researches and Engineering Journal (IAREJ) and the Author(s).

1. Introduction

A number of fine results have been obtained by some numerical electric field computations methods that have been greatly improved during recent years. Numerical electric field computation is now indispensable to the designing of high voltage power transformer bushings and other insulated apparatus from the viewpoint of reliability and reduction in size of apparatus [1]. In the case of designing SF₆ gas insulated apparatus, the field calculation has special meaning of importance because the insulation characteristics of SF₆ gas greatly depend on the electric field strength [2]. As well as to analyze the field a number of efforts have recently been made to obtain optimum electrode profiles having minimum and uniform electric field [3, 4].

The main purpose of electric field optimization is to obtain uniform electric field distribution as well as to minimize the field strength on the electrode surface [5]. This enables one to make the best use of the electric field space, reducing the size of high voltage power transformer

bushings and other insulated apparatus. Electric field calculations by numerical techniques is to use different numerical techniques to find electric field distributions, which are inevitable tool in various electricity concerned technologies [6]. Up to now, several 3D dimensional electrode profiles with quasi-uniform electric field have been obtained using conformal mapping and experiments. They are noted as a finite difference method profile and finite element method profile [7, 8].

The examined electrode systems are modeled as 2D using axial symmetry. In this approach, it is considered that 3D electric field distribution is obtained by rotating 2π radians around the symmetry axis of the models. Among them is the finite difference method profile which has a completely uniform electric field along the electrode surface. However, this complete electric field uniformity will disappear if this profile is applied to a 3D dimensional axisymmetric electrode.

Huang et al. and Hyouk et al. calculated electric field distribution of the two dimensional finite difference

* Corresponding author. Tel.: +90-372-291-2617

E-mail addresses: nihatpamuk@beun.edu.tr; nihatpamuk@gmail.com (N. Pamuk)

ORCID: 0000-0001-8980-6913 (N. Pamuk)

DOI: 10.35860/iarej.765360

This article is licensed under the CC BY-NC 4.0 International License (<https://creativecommons.org/licenses/by-nc/4.0/>).

method profile and 3D dimensional axisymmetric finite difference method profiles to evaluate the discrepancy from the uniformity for the latter profiles. Furthermore, by using the computation program for high voltage electric field automatic optimization, a new uniform field electrode profile was obtained as a replacement of the 3D dimensional finite difference method profile. Other optimum 3D dimensional axisymmetric electrode profiles are also obtained which are enclosed with metallic coaxial cylinder [9, 10].

Most of the studies found that there was electrostatic field calculation and optimization structure in power transformer bushing insulation, while some studies such as [11, 12] found that there was condition assessment of high voltage bushing with solid insulation structure. Some studies such as [13, 14] have found that electromagnetic forces and losses computation and design of power transformer bushings. By applying theory of electric field optimization based on charge simulation method, the author developed a computation program for electric field automatic optimization of an electrode profile with 3D dielectrics in axisymmetric field.

The purpose of this paper is to make the radial stiffness characteristic of the given 3D rubber bushing model meet the target stiffness curve by using the optimization method presented in this paper. In order to determine the stiffness curve of the bushing, nonlinear finite model was defined using boundary conditions.

2. Basic Equations for the Method of Optimization

The charge simulation method is made up of the following basic equation. To simplify of discussion, the author consider one dielectric field problem.

$$[P] \cdot \{Q\} = \{\phi\} \quad (1)$$

In equation 1, P is a potential coefficient matrix determined by coordinates of contour point and charge point. Q is a charge vector. ϕ is a potential vector of contour points. In general, P and ϕ are given, thus providing the value of Q. From the value of Q, the author can calculate the electric field strength. [15, 16] proposed that electric field should be improved by properly arranging several new charges (optimizing charges) in the field obtained by charge simulation method. Let Q' be an optimizing charge vector.

$$[P] \cdot \{Q\} + [P'] \cdot \{Q'\} = \{\phi\} \quad (2)$$

In equation 2, P' is a matrix of varied part of potential coefficients determined by arrangement of new optimizing charges. Combining with the given value Q', the value Q obtained by equation 2 determines the electric field distribution along a new electrode. The profile of a new electrode is obtained as a locus of equipotential line of electrode potential. If the electric field on a new electrode surface does not distribute as uniformly as expected, the

above computation is iterated by giving new Q' to equation 2 [17, 18, 19].

This computation is iterated until uniform field distribution of electrode surface is obtained. For a good convergence and satisfactorily uniform potential distribution, it is important to determine the value of Q' appropriately. This is discussed in the following section. On the other hand, the basic equation of the charge simulation method in two electrostatic dielectric field may be generally expressed by equation 3.

$$\begin{bmatrix} P \\ F \end{bmatrix} \cdot [Q] = \begin{bmatrix} \phi \\ 0 \end{bmatrix} \quad (3)$$

In equation 3, F is an electric field coefficient matrix determined by dielectric boundary points. Like equation 2, equation 3 is modified by arranging new optimizing charges Q', as follows equation 4.

$$\begin{bmatrix} P \\ F \end{bmatrix} \cdot [Q] + \begin{bmatrix} P' \\ F' \end{bmatrix} \cdot [Q'] = \begin{bmatrix} \phi \\ 0 \end{bmatrix} \quad (4)$$

In equation 4, F' is a matrix of varied part of electric field coefficients determined by arrangement of optimizing charges. Like in one dielectric field, electrode surface electric field can be optimized also in two dielectric field, using equation 4.

3. Automatic Optimization Technique

The author succeeded in obtaining the optimized electric field distribution by using iterative computation by arranging vector (Q') automatically. In each iteration step, Q' is given to correct local maximum and minimum of the electric field distribution along the electrode profile [20]. This method is described along with a model for consideration in Figure 1.

In Figure 1, A-G is an electrode profile to which optimization is to be applied. Other parts of the profile do not vary through the iterative computation since these points are always fixed as the contour points. Optimizing charge vector (Q'₁) given at an initial time is arranged at a positions shown by symbol ●. The electrode profile calculated (solid curve) is identical to the equipotential surface. The electric field distribution in A-G is expressed by solid curve shown in Figure 2.

This curve provides local maximum points at B, D, F and local minimum points at C and E. To correct this electric field distribution, new charges (optimizing charges) are arranged at the vicinity of A, C and E. (shown by symbol ◼) Figure 3 shows a detail of arrangement of an optimizing charge. Taking point C as an example, the author arrange the optimizing charge Qc' at point S away from point C by distance ℓ_{cs} . ℓ_{cs} may be expressed by equation 5.

$$\ell_{CS} = k \cdot \text{Min} (\ell_{BC}, \ell_{CD}) \quad (5)$$

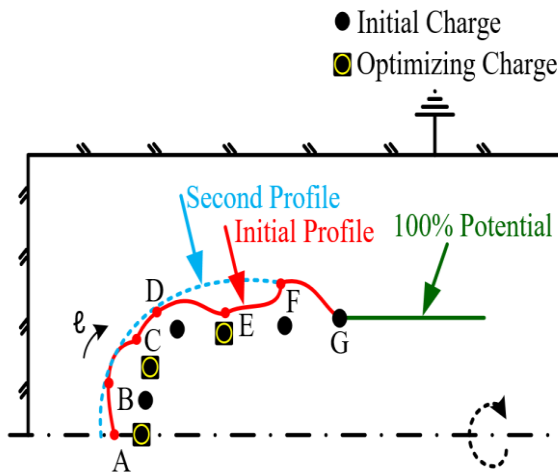


Figure 1. Optimization of electrode profile

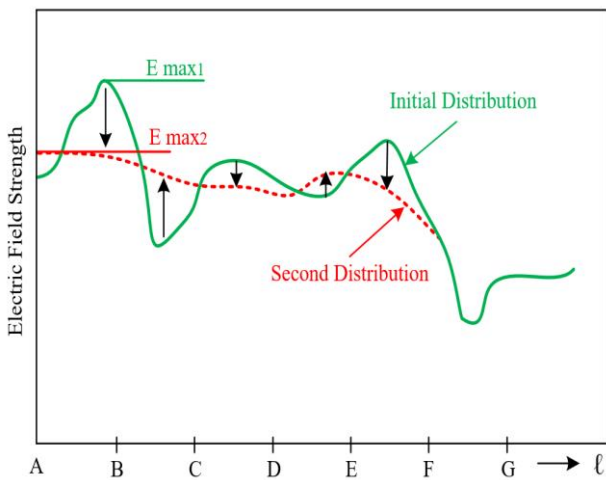


Figure 2. Electric field strength distribution

In equation 5, k gives an appropriate value of $1 \leq k \leq 2$. The value of Q_c' is determined by equation 6 using potential value jV_{CB} and jV_{CD} , which are given by a function f in equation 7, where E_j is an electric field strength on next following point j .

$$Q_c' = (*) \cdot \frac{v}{j} (P_{cj}^{-1} \cdot jV_{cj}) \quad (j = B, D) \quad (6)$$

$$jV_{cj} = f \cdot (|E_j - E_c|) \quad (j = B \text{ or } D) \quad (7)$$

In equation 6, P_{cj} is a potential coefficient, and $*$ is the relaxation factor which is introduced in order to get smooth convergence of iterative computation. The value of $*$ depends on the electrode profile. Let (Q'_2) be a newly given vector by the above procedure, the equipotential surface (new electrode surface) shown by dotted line in Figure 1 is obtained. The corresponding electric field distribution is shown by dotted line in Figure 2. The above calculation process is automatically iterated and the electrode profile with the optimized electric field distribution is obtained by judging the convergence from a reduction rate of the maximum electric field and an achievement of uniformity of electric field distribution.

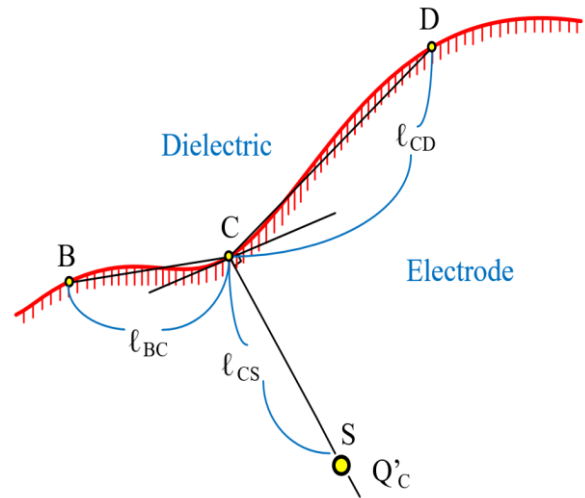


Figure 3. Arrangement of optimizing charge

4. Examples of Optimized Electrode Profile

This section gives some calculation examples using above mentioned computation program for optimization. Figure 4 shows an example of the end profile of high voltage conductor in a ground potential cylindrical enclosure. Figure 4 indicates an electrode profile at the initial stage with optimizing charge positions, while Figure 5 shows those as a result of automatically iterative calculation of five times.

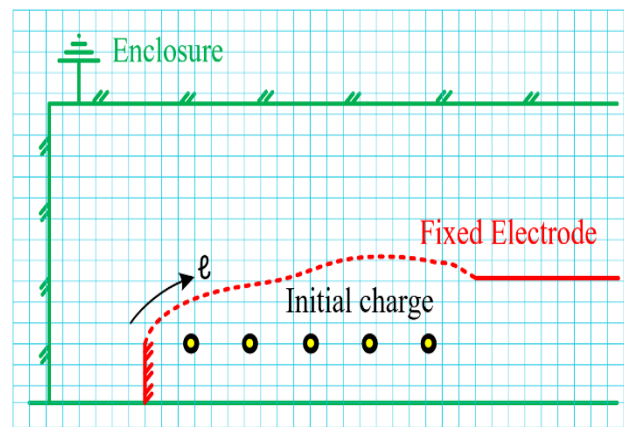


Figure 4. Initial electrode profile

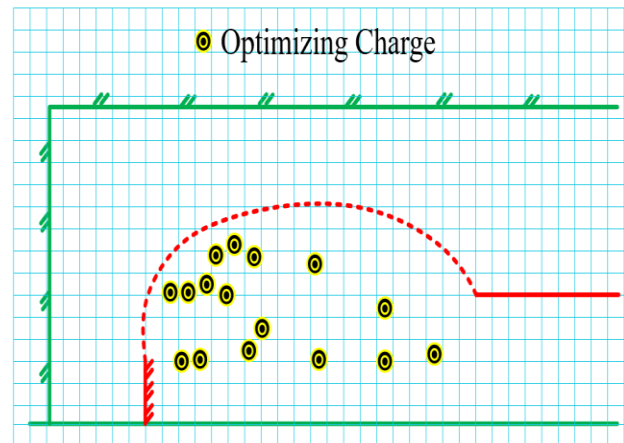


Figure 5. Optimized electrode profile

Figure 6 shows a variation of electric field distribution. The iterative calculation reveals an obvious reduction of the maximum electric field strength and a uniformity of electric field distribution.

Figure 7 shows further example of optimized profile of another type conductor end in grounded cylindrical enclosure, and the electric field distribution along it. Optimized profile and electric field distribution obtained with and without the insulating cylinder in high voltage power transformer bushing are given in Figure 8 for comparative study.

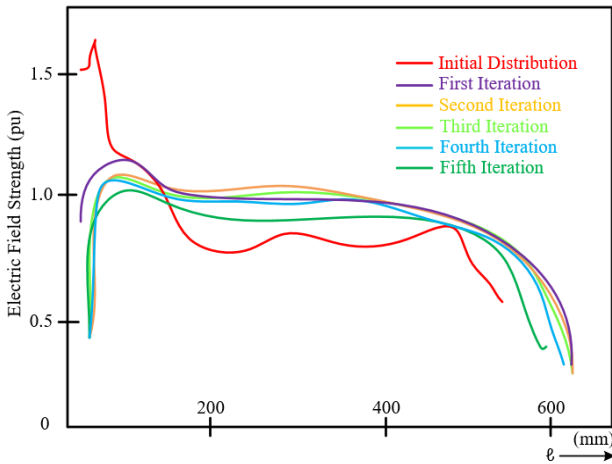


Figure 6. Electric field distribution

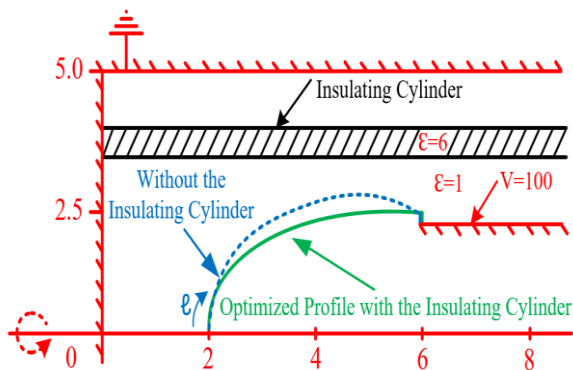


Figure 7. Optimized profile with and without insulating cylinder

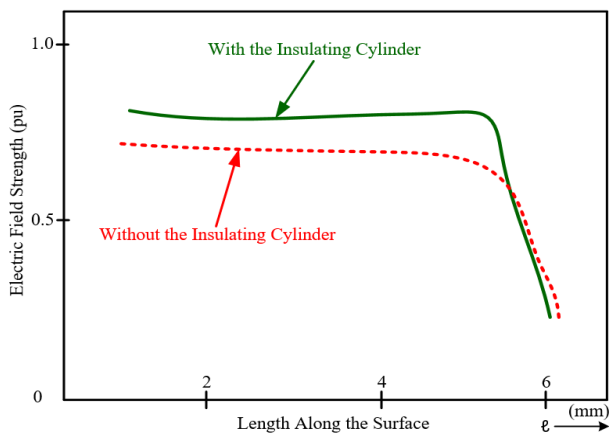


Figure 8. Electric field distribution with and without insulating cylinder in high voltage power transformer bushing

5. 3D Dimensional Electrode Profile

3D dimensional electrode profile ($\pi/2$ dimensional profile) against infinite plane may be expressed as follows by using parameter φ . (Point A is assumed as an origin.)

$$x = -2 \left[\sin\varphi - \ell \tan\left(\frac{\varphi}{2} + \frac{\pi}{4}\right) \right] \quad (\varphi = 0 - \frac{\pi}{2}) \quad (8)$$

$$y = 2[1 - \cos\varphi] \quad (\varphi = 0 + \frac{\pi}{2}) \quad (9)$$

$$z = 2 \left[\sin\varphi + \ell \tan\left(\frac{\varphi}{2} - \frac{\pi}{4}\right) \right] \quad (\varphi = 0) \quad (10)$$

Figure 9 illustrates 3D dimensional electrode profile with 100% potential. The grounded infinite plane electrode is located at $x = 2-\pi$, $y = 2+\pi$ and the gap length is π as $z \rightarrow \infty$. Arrows in Figure 9 drawn by computer show electric field vectors on the 3D dimensional electrode profile.

The electric field strength is calculated by using charge simulation method. The results reveal that the electric field distribution on 3D dimensional electrode profile is completely uniform. The author apply the 3D dimensional electrode profile to an axisymmetric electric field distribution. One may consider an end portion profile of a rod electrode. The problem is, however, that this 3D dimensional electrode profile loses the uniformity of the electric field distribution along the profile by influence of axial curvature and that electric field strength increases as going apart from the axis. By using charge simulation method, the author calculated the discrepancy of the electric field uniformity. Figure 10 shows the result as a function of 3D coordinate, where (x_0, y_0, z_0) is the coordinate of edge point A assuming the axis center of the infinite plane as origin.

Minimum electric field strength E_{min} is obtained on the center axis of the 3D dimensional electrode profile, while the maximum electric field strength E_{max} is obtained on point A. Figure 10 reveals that the discrepancy from the uniformity of electric field is 10% or more if $|x_0/y_0/z_0| < 5$ and 5% or more if $|x_0/y_0/z_0| < 10$. In other words, 2D dimensional electrode profile directly applied to 3D dimensional axisymmetric field cannot be used as an insulation breakdown test. The fatal problem is that insulation breakdown is expected to occur at edge point A of this electrode.

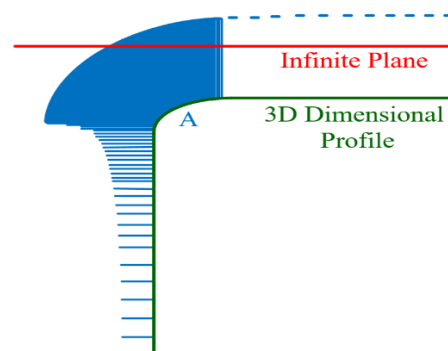


Figure 9. 3D dimensional profile and electric field distribution

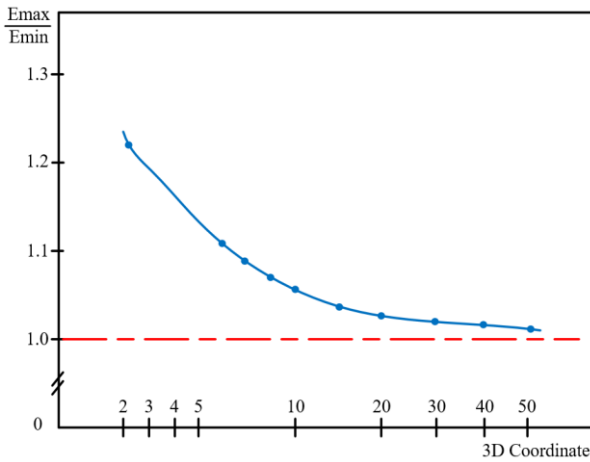


Figure 10. Discrepancy from the electric field uniformity

6. Optimized Profile in Axisymmetric Field

First of all, the parameter values of the elastoplastic transformer bushing model were obtained by using the finite difference analysis method. With the experiments applied in the design phase, the bandwidths of the hysteresis curve were determined by fitting the curve model obtained as a result of the least squares regression method. The software values of the hysteresis curve obtained as a result of the finite difference analysis take into account the damping force and curve bandwidth values. Thus, both viscoelastic and elastoplastic components are represented. In addition, the slope value of the hysteresis curve shows the decreased stiffness value due to the amplitude effect and its behavior is represented by the elastoplastic component value.

The rubber structured transformer bushing sample was modeled based on the geometric structure of the finite difference analysis. It is ensured that the boundary condition value of the finite difference analysis model, the constant condition value on the outer flange of the transformer bushing and the displacement value applied to the inner rod element of the bushing at the central point are the same as the experimental conditions. Rotational hardness information was obtained by applying torque from 0 Nmm to 6000 Nmm in the x direction and from 0 Nmm to 600 Nmm in the y and z direction, respectively. Rotational stiffness tests were not conducted due to the limited number of experimental devices. For this reason, the values obtained by simulation based on finite difference analysis values were used.

The electric field on the 2D dimensional electrode profile applied to 3D dimensional axial symmetry does not meet requirements of uniform electric field distribution. The author calculated a new uniform electric field electrode profile by using charge simulation program for electric field automatic optimization. Figure 11 shows a part of the results and has been obtained by iterative computation with a starting value of 3D dimensional electrode profile when $|x_0/y_0/z_0| = 4$. The distortion of surface electric field strength is less than 0.4% if $|x| < 3.5$ and the strength slightly reduces

in the vicinity of the point A.

This new electrode profile is most appropriate to one for an insulation breakdown testing because uniform electric field strength is realized on a wide electrode area and the electric field decreases as going apart from the uniform field region. The author discussed the case where a high voltage rod electrode is in a cylindrical grounded enclosure. The author obtained uniform electric field distribution of the end portion from many trials with various distances from the enclosure wall. Figure 12 shows the result, and D_i is a diameter of the rod electrode D_0 an inner diameter of the grounded enclosure.

Also, G is a gap length at the rod end portion center. Assuming that $G = 1$ and $D_i = 20$, the author obtained the optimum electrode profile as a function of D_0 . If $D_0 = 22.104$, the uniform electric field spreads over the entire electrode surface. If D_0 is larger, the uniform electric field is obtained only at the top end portion of the electrode. If $D_0 = \infty$, the profile is identical to the profile optimized from 3D dimensional electrode profile previously discussed. Figure 12 shows that there is almost no variation in the optimum profile if $D_0 \geq 30$, meaning that the grounded enclosure wall does not so much affect the electric field on the electrode surface.

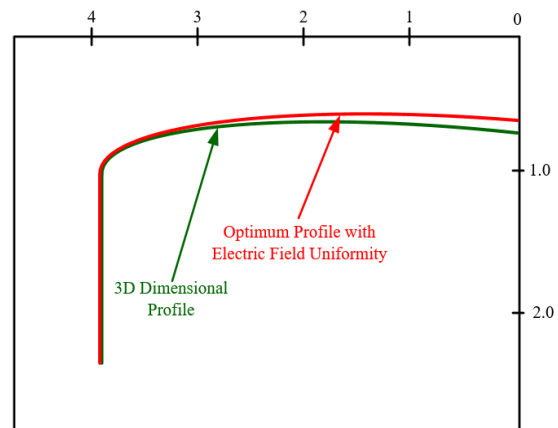


Figure 11. Axisymmetric 3D dimensional electrode profile with electric field uniformity

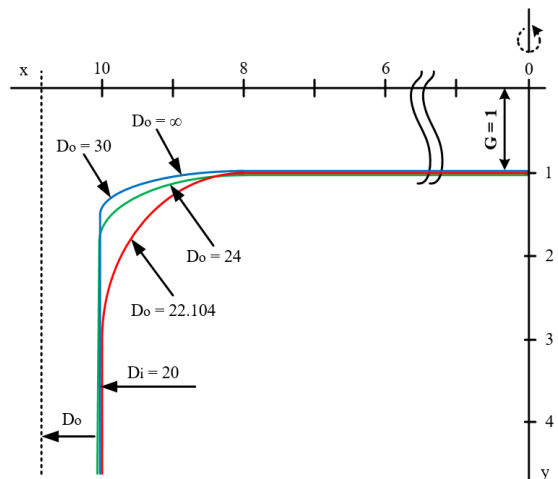


Figure 12. Optimized electrode profile with cylindrical enclosure

7. Conclusions

Satisfactory results were obtained from the computation program for electric field automatic optimization in high voltage power transformer bushing developed by applying charge simulation theory of electric optimization. In above mentioned simulation program, the main feature is that new charges are arranged consecutively in order to correct the variation in electric field distribution of the electrode surface, thus making it possible to achieve the electric field uniformity by automatic iterative computation. Electric field calculation using charge simulation method performed for a 2D dimensional electrode profile revealed that the uniformity of electric field strength distribution along it is completely obtained.

Extended 3D dimensional electrode profile to a 3D dimensional axisymmetric field does not have an electric field uniformity any longer. Deviation from the uniformity was calculated by charge simulation method, and it has been clarified that the smaller the electrode diameter and the larger the distortion electrode diameter. In axisymmetric 3D dimensional field, the computation program for electric field automatic optimization developed by the author realized a new electrode profile that provides a uniform electric field distribution. Such electrode is suitable for an insulation breakdown testing as a replacement of the 3D dimensional electrode profile. The computation for electric field optimization on a rod electrode in a grounded cylindrical enclosure provided the optimized electrode profile as a function of enclosure diameter. If the inner diameter of grounded enclosure is 30 or more there is almost no variation in optimized configuration for a rod electrode of a diameter of 20 for a gap length of 1.

Declaration

The author declared no potential conflicts of interest with respect to the research, authorship, and/or publication of this article. The author also declared that this article is original, was prepared in accordance with international publication and research ethics, and ethical committee permission or any special permission is not required.

Author Contributions

N. Pamuk is responsible for all section of the study.

References

1. El-Makkawy, S.M. El-Dessouky, S.S., *Analytical Aspects in the Presence of Polymeric Materials in Field Gaps of HV Insulation System*, Proceedings of 8th International Symposium on Electrets (ISE 8), 06 August 2002, Paris, France, p. 905-910.
2. Weifang, J. Huiming, W. Kuffell, E., *Application of the Modified Surface Charge Simulation Method for Solving Axial-symmetric Electrostatic Problems with Floating Electrodes*, Proceedings of 4th International Conference on Properties and Applications of Dielectric Material, 1994, Brisbane, Qld, Australia, p. 28-30.
3. Abidaoun, H.S. Maather, A.I. Mohanad, H.A. Saad, Q.F., *Estimation and Plot of Electrical Field Using Finite Difference Method*, Second Engineering Scientific Conference College of Engineering, 16-17 December 2015, University of Diyala, p. 501-510.
4. Vahidi, B., Mohammadzadeh Fakhr Davood A., *Application of charge simulation method to electric field calculation in the power cables*. Iranian Journal of Science & Technology, Transaction B, Engineering, 2006. **30**(B6): p 789-794.
5. Hu, R. Zhang, Z. Wang, S. Lu, Y. Liu, L. Zhu, S. Peng, Z., *Electric Field Optimization of Cast Resin Dry-Type Transformer Under Lightning Impulse*, IEEE Conference on Electrical Insulation and Dielectric Phenomena (CEIDP), 20-23 October 2019, Richland, USA, p. 556-559.
6. Biswanath, M., *Electric field calculations by numerical techniques*, Bachelor Thesis in Electrical Engineering 2009, National Institute of Technology Rourkela, India. p. 6-7.
7. Zhou, K., Ivanco, A., Filipi, Z., Hofmann, H., *Finite element based computationally efficient scalable electric machine model suitable for electrified powertrain simulation and optimization*. IEEE Transactions on Industry Applications, 2015. **51**(6): p 4435-4445.
8. Lee, K.H., Hong, S.G., Baek, M.K., Choi, H.S., Kim, Y.S., Park, I.H., *Alleviation of electric field intensity in high voltage system by topology and shape optimization of dielectric material using continuum design sensitivity and level set method*. IEEE Transactions on Magnetics, 2015. **51**(3): p. 1-4.
9. Huang, Y., Xu, Q., Tan, Q., Xie, N., *Optimization of electric field distributions in OVS with hybrid algorithm*. IEEE Sensors Journal, 2019. **19**(21): p 9748-9754.
10. Hyouk Lee, K., Geon Hong, S., Ki Baek, M., Soon Choi, H., Sun Kim, Y., Han Park, I., *Adaptive level set method for accurate boundary shape in optimization of electromagnetic systems*. COMPEL The International Journal for Computation and Mathematics in Electrical and Electronic Engineering, 2014. **33**(3): p. 809-820.
11. Du, B., Sun, H., Jiang, J., Kong, X., Yang, W., *Temperature dependent electric field distribution in ± 800 kV valve-side bushing insulation for a converter transformer*. High Voltage, 2020.
12. Subocz, J., Mrozik, A., Bohatyrewicz, P., Zenker, M., *Condition assessment of HV bushings with solid insulation based on the SVM and the FDS methods*. Energies, 2020. **13**(4): 853, p. 1-13.
13. Li, Z., Yujiao, Z., Guanteng, X., Jiansheng, Y., Lan, J., *Electrostatic field calculation and structure optimization of new shield ring of 1000 kV Nan-Jing loop transmission line*. Transactions on Electrical and Electronic Materials, 2020. p. 1-8.
14. Al-Abadi, A. Gamil, A. Schatzl, F., *Optimization of Magnetic Shunts Towards Efficient and Economical Power Transformers Design*, Proceedings of the 21st International Symposium on High Voltage Engineering, 28 November 2019, ISH2019, p. 15-26.
15. Cao, Y., Liu, X., Wang, E., Jin, L., Wang, G., *Electric field optimization design of a vacuum interrupter based on the tabu search algorithm*. IEEE Transactions on Dielectrics and Electrical Insulation, 2002. **9**(2): p 169-172.
16. Zhao, Y.N., Zhang, G.Q., Guo, Z.Z., Cheng, S., *The mathematical model of electrical field distribution in optical voltage transformer*. Procedia Engineering, 2012. **29**(1):

p.2661-2666.

17. Tan, Q., Xu, Q., Chen, L., Huang, Y., *A new method to improve internal electric field distributions of poekels OVS*. IEEE Sensors Journal, 2017. **17**(13): p 4115-4121.
18. Wang, S., Kang, J., *Shape optimization of BLDC motor using 3D finite element method*. IEEE Transactions on Magnetics, 2000. **36**(4): p. 1119-1123.
19. Okamoto, Y., Masuda, H., Kanda, Y., Hoshino, R., Wakao, S., *Convergence acceleration of topology optimization based on constrained level set function using method of moving asymptotes in 3D nonlinear magnetic field system*. IEEE Transactions on Magnetics, 2017. **53**(6): p. 1-4.
20. Ho, S.L., Chen, N., Fu, W.N., *A moving mesh embedded algorithm in finite element method for optimal design of electromagnetic devices*. IEEE Transactions on Magnetics, 2011. **47**(10): p. 2947-2950.